Influence of oxygen content on the structural, magnetotransport, and magnetic properties of LaMnO$_{3+\delta}$

C. Ritter

Institute Laue-Langevin, Boîte Postale 156, 38042 Grenoble, Cedex, France

M. R. Ibarra,[*] J. M. De Teresa, P. A. Algarabel, C. Marquina, J. Blasco, and J. García
Departamento de Física de la Materia Condensada and Instituto de Ciencia de Materiales de Aragón, Universidad de Zaragoza and Consejo Superior de Investigaciones Científicas, Facultad de Ciencias, 50009-Zaragoza, Spain

S. Oseroff
Physics Department, San Diego State University, San Diego, California 92108

S-W. Cheong
Bell Laboratories, Lucent Technologies, 700 Mountain Avenue, Murray Hill, New Jersey 07974

A systematic study of the effect of oxygen content on the structural, magnetotransport, and magnetic properties has been undertaken on a series of LaMnO$_{3+\delta}$ samples, with $\delta = 0$, 0.025, 0.07, 0.1, and 0.15. Measurements of the ac initial magnetic susceptibility, magnetization, magnetoresistance, and neutron diffraction, including small-angle neutron scattering (SANS), were performed in the temperature range 1–320 K using high magnetic fields up to 12 T. The antiferromagnetic order found in LaMnO$_3$ evolves towards a ferromagnetic order as δ increases. This behavior is accompanied by a drastic reduction of the static Jahn-Teller distortion of the MnO$_6$ octahedra. The ferromagnetic coupling weakens for $\delta \gtrsim 0.1$. The magnetic behavior is interpreted by taking into account two effects caused by the increase in δ: cation vacancies and Mn^{4+}/Mn^{3+} ratio enhancement. The orthorhombic crystallographic structure becomes unstable at room temperature for $\delta \gtrsim 0.1$. The sample $\delta = 0.1$ shows a structural transition from rhombohedral to orthorhombic below $T_S \approx 300$ K with a huge change in the cell volume. All the studied compounds were found to be insulating at low temperatures with no appreciable magnetoresistance, except for $\delta = 0.15$, in which we observed a large value for the magnetoresistance. The SANS results indicate that magnetic clustering effects are important below T_C for $\delta \gtrsim 0.07$, which could explain the intriguing ferromagnetic insulator state. In the $\delta = 0.07$ and $\delta = 0.10$ samples we found at temperatures below T_C magnetic and structural anomalies that are characteristic of charge ordering. [S0163-1829(97)04837-6]

I. INTRODUCTION

The renewed interest in the mixed-valence manganese oxide perovskites, due to their unusual magnetoresistive properties, has stimulated us to carry out a detailed study of the possible causes that give rise to this behavior. The presence of Mn^{4+} is recognized as necessary for the metallic character found in these compounds when ferromagnetic. The existence of Mn^{4+} can be achieved by the substitution of La by a divalent ion such as (Ca^{2+}, Sr^{2+}, Ba^{2+}).[1–3] Nevertheless, as pointed out by Toffield and Scott,[4] LaMnO$_{3+\delta}$ is the only system in the lanthanum-transition-metal perovskites which exhibits a wide range of oxidative nonstoichiometry. These authors argued that the excess of oxygen cannot be accommodated interstitially in the lattice. Thus, they postulated the existence of La and Mn vacancies. Roosmalen and Cordfunke,[5] after a careful study of several nonstoichiometric compounds using neutron diffraction, concluded that the oxygen excess δ results in *equivalent* amounts of La and Mn vacancies. Therefore, LaMnO$_{3+\delta}$ is not necessarily correct as one should write La$_{3/(3+\delta)}$Mn$_{3/(3+\delta)}$O$_3$. However, for the sake of simplicity, we will use the nomenclature LaMnO$_{3+\delta}$ in

this paper, the percentage of Mn^{4+} being obtained as % Mn$^{4+} = 2 \times 100\delta$. Recent neutron-diffraction experiments on La$_{1-t}$MnO$_{3+\delta}$ by Hauback, Helmer, and Sakai[6] have characterized the role of La vacancies in relation to the oxygen excess. They proposed the existence of three different crystallographic structures ORT1 (orthorhombic with a large Jahn-Teller distortion of the MnO$_6$ octahedra), ORT2 (orthorhombic with a very small Jahn-Teller distortion), and RH (rhombohedral structure). Concerning the magnetic and magnetotransport properties of the nonstoichiometric compounds, for high values of δ, Rao and Cheetham[7] and Mahendiran *et al.*[8] found low-temperature ferromagnetic order together with a metal-insulator transition and large magnetoresistance. This was supported by subsequent neutron-diffraction experiments by Cheetham *et al.*[9] Recently, the role of the La and Mn vacancies in La$_{1-t}$MnO$_3$ and LaMn$_{1-t}$O$_3$ was carefully studied by Arulraj *et al.*[10] From these studies, it was established the existence of a pseudocubic crystallographic phase when the number of vacancies at the Mn sites reaches a value of 10%. Moreover, this number of vacancies is enough to destroy the ferromagnetism.[10] The aim of the present work is to carry out a systematic study of

TABLE I. Data of the magnetic behavior for all the studied compounds.

δ	0	0.025	0.07	0.1	0.15
Mn^{4+} (%)	0	5	14	20	30
Formula unit	$LaMnO_3$	$La_{0.992}Mn_{0.992}O_3$	$La_{0.977}Mn_{0.977}O_3$	$La_{0.968}Mn_{0.968}O_3$	$La_{0.952}Mn_{0.952}O_3$
Magnetic order	AF $T_N = 140$ K	F+AF $T_C = 110$ K F 1.48	F+AF $T_C = 160$ K F 3.25	F $T_C = 150$ K	F $T_C = 160$ K
μ (μ_B)	3.49	2.92 AF 2.52	3.26 AF 0.25	2.86	0.78
Paramagnetic region					
C (emu K/mol)	3.48	5.38	4.34	4.45	4.66
θ_P (K)	46	126	171	170	129
μ_{eff}	5.3	6.6	5.9	6.0	6.1
Ferromagnetic region					
M_S (5 K, $H = 0$) (emu/mol)	624.4	3919.5	19 181	17 046	5421.2
$\Delta M / \Delta H$ (5 K) (emu/mol Oe)	2.7×10^{-2}	4.86×10^{-2}	6.9×10^{-3}	2.3×10^{-2}	0.97×10^{-2}
μ_{eff}	0.11	0.70	3.43	3.05	0.97

the effect of Mn^{4+} in $LaMnO_{3+\delta}$ ($\delta \leqslant 0.15$), i.e., with an equal number of La and Mn vacancies, in order to investigate the crossover from antiferromagnetism and orthorhombic structure for $\delta = 0$ to ferromagnetism and rhombohedral structure. Special care was given to the sample preparation and the subsequent chemical analysis. We have studied two batches of samples. One batch was prepared at the Bell Laboratories, Lucent Technologies ($\delta = 0$, 0.07, 0.15) and another one with additional intermediate concentrations ($\delta = 0.025$, 0.1) at the Instituto de Ciencia de Materiales de Aragón. We report magnetotransport, magnetic, and neutron-diffraction measurements, including small-angle neutron scattering, which will allow us to investigate the evolution of the crystallographic and magnetic properties along the series.

II. EXPERIMENTAL RESULTS

The samples were prepared following a solid-state reaction method starting from stoichiometric amounts of La_2O_3 and Mn_2O_3. The samples $\delta = 0$, 0.07, and 0.15 were prepared and heat treated at the Bell Laboratories, Lucent Technologies. The starting samples $LaMnO_{3+\delta}$ were obtained by heating the starting materials in air at 1250 °C for 5 h, at 1380 °C for 12 h, and at 1390 °C for 20 h with intermediate grindings. The sample $\delta = 0$ was obtained by annealing in Ar atmosphere at 1000 °C. The sample $\delta = 0.07$ was obtained as prepared. Finally the $\delta = 0.15$ sample was annealed under an oxygen pressure of 200 bars. The samples $\delta = 0.025$ and 0.1 were prepared and heat treated at the Instituto de Ciencia de Materiales de Aragón: the starting stoichiometric amounts of La_2O_3 and Mn_2O_3 were mixed and calcined at 1000 °C in air overnight, then ground, pressed and sintered at 1250 °C for 48 h with intermediate grindings. The sample $\delta = 0.025$ was annealed at 1000 °C for 12 h in a current flow of nitrogen and the sample $\delta = 0.1$ in a flow of oxygen with the same conditions (1000 °C/12 h). Some samples with the same

oxygen content that those prepared at the Bell Laboratories were also prepared at the Instituto de Ciencia de Materiales de Aragón and they showed the same physical properties. The Mn^{4+} content in the samples was determined by redox titration analysis by using titrated potassium permanganate solution (see Table I). X-ray-diffraction patterns from 18° up to 100° in steps of 0.02° were collected by using a Rigaku D/max-B instrument with a copper rotating anode. The refinement of the data confirmed the quality of our samples, in which an equal number of La and Mn vacancies were obtained within the experimental error. The resistivity was measured using a standard four-point method and the magnetoresistance up to 12 T using a superconducting coil. Magnetic measurements, ac initial susceptibility, and dc magnetization, were carried out by using a commercial Quantum Design superconducting quantum interference device magnetometer between 5 and 300 K and magnetic fields up to 5 T. Neutron-diffraction experiments were performed at the high flux reactor of the ILL. The D1B instrument was used for the thermal scan using a wavelength $\lambda = 2.52$ Å and covering an angular range $2° \leqslant 2\theta \leqslant 80°$. The high-resolution D2B instrument with a $\lambda = 1.59$ Å was used to obtain more accurate values of the structural parameters at selected temperatures. The small-angle scatering (SANS) instrument D16 was used to study the SANS magnetic contribution at low transfer moment values 0.03 Å$^{-1} \leqslant q \leqslant 0.65$ Å^{-1}.

A. Electrical resistivity

The electrical resistivity was measured for selected compounds within the temperature range 4–300 K. The results are shown in Fig. 1. An activated semiconducting-type behavior is observed through the whole series in agreement with previous results.[11] The magnetoresistance was found to be negligible for all the compounds except for the sample $\delta = 0.15$, where a change in four orders of magnitude in the
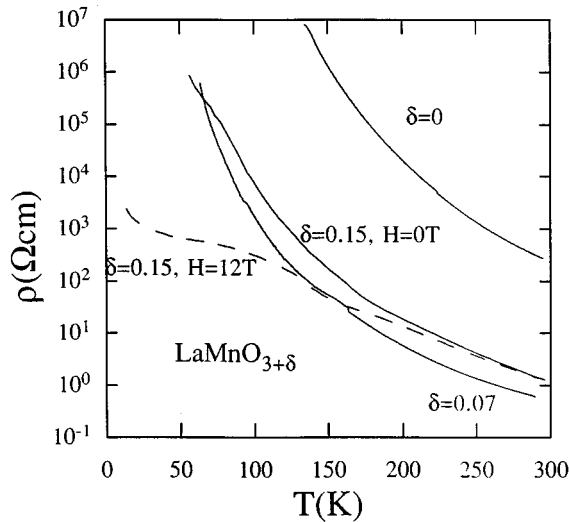
FIG. 1. Thermal dependence of the resistivity of the compounds LaMnO$_{3+\delta}$. Appreciable magnetoresistance ratios have been found only in the $\delta=0.15$ compound.

resistivity at 12 T was found. Our samples do not show a spontaneous or field-induced metal-insulator transition.

B. Magnetic measurements

The initial ac susceptibility χ_{ac} was measured to obtain the temperature of the magnetic order transition. The compound $\delta=0$ shows a very weak but well-defined peak at $T_N=140$ K. At this temperature a para-antiferromagnetic ordering transition takes place [see inset of Fig. 2(a)]. As δ increases, we can observe in Fig. 2(a) a dramatic change in the thermal dependence of χ_{ac}, which is associated with the enhancement of the ferromagnetic interaction. The transition temperatures obtained from these measurements are given in Table I. For all the compounds the increase in χ_{ac} starts at temperatures of about 160 K, the largest anomaly being observed for $\delta=0.07$. In the $\delta=0.07$ and $\delta=0.1$ samples an abrupt decrease in χ_{ac} takes place at around 110 K. This remarkable effect resembles that found in (La-Ca)MnO$_3$ at the charge-ordering temperature.[12] To better characterize the magnetic behavior, we measured magnetization versus field. In Fig. 2(b) we present, for 4 K, the data for all the studied samples. The magnetization isotherms for the compounds $\delta=0.07$ and $\delta=0.1$ display a characteristic ferromagneticlike behavior. From these data we obtain values for the effective magnetic moment of the Mn ion of $3.43\mu_B$ and $3.05\mu_B$ for $\delta=0.07$ and $\delta=0.1$ samples, respectively (see Table I). The $\delta=0.025$ sample has a very small ferromagnetic moment, $0.7\mu_B$. This small value can be an indication of the existence of a canted antiferromagnetic structure or the coexistence of ferro and antiferromagnetic regions at low temperatures. The high-field susceptibility observed for this compound is close to that found in LaMnO$_3$. The origin for this weak ferromagnetic contribution in the compound $\delta=0$ is still not understood. As we will see in the next section, neutron-diffraction results do not show any spontaneous ferromagnetic contribution. Consequently, the weak ferromagnetic component $(0.1\mu_B)$ may be ascribed either to a small intersublattice canting induced by the applied magnetic field
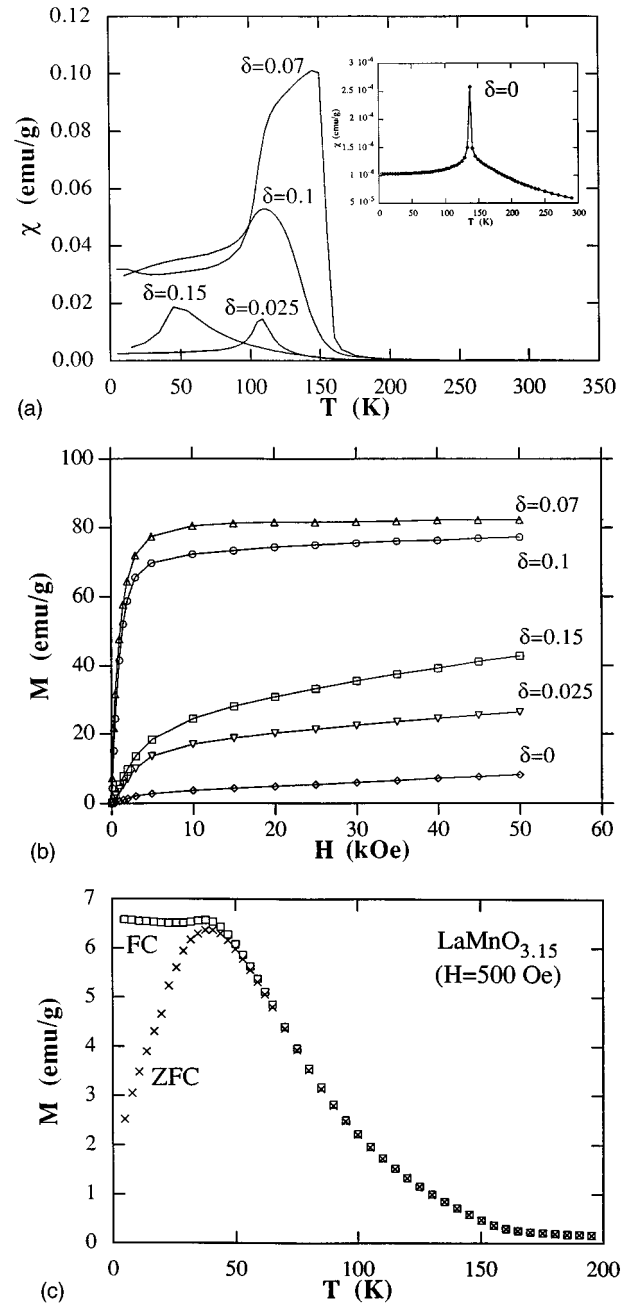

FIG. 2. (a) Thermal dependence of the χ_{ac} of the compounds LaMnO$_{3+\delta}$. The inset shows the χ_{ac} of LaMnO$_3$. (b) Magnetization isotherms of the LaMnO$_{3+\delta}$ compounds at 5 K. (c) Thermal dependence of the magnetization of LaMnO$_{3.15}$ under an applied magnetic field of 500 Oe for increasing temperatures after cooling the sample in zero-field (ZFC) or under a field of 500 Oe (FC).

or to the presence of very small amount of Mn^{4+} $(\delta\lll)$, not detectable by our analysis probes. Under this assumption, the high-field susceptibility in the compound $\delta=0.025$ should also have this origin. However, in this case there exists a spontaneous canting between the antiferromagnetic coupled sublattices $(0.7\mu_B)$. This assumption is in agreement with the neutron-diffraction results as we will see in the next section. We have observed an enhancement of the ferromagnetic interaction as δ increases. Nevertheless, the compound $\delta=0.15$, with the largest δ value, has a very low value of the ferromagnetic moment $(0.97\mu_B)$. This peculiar behav-
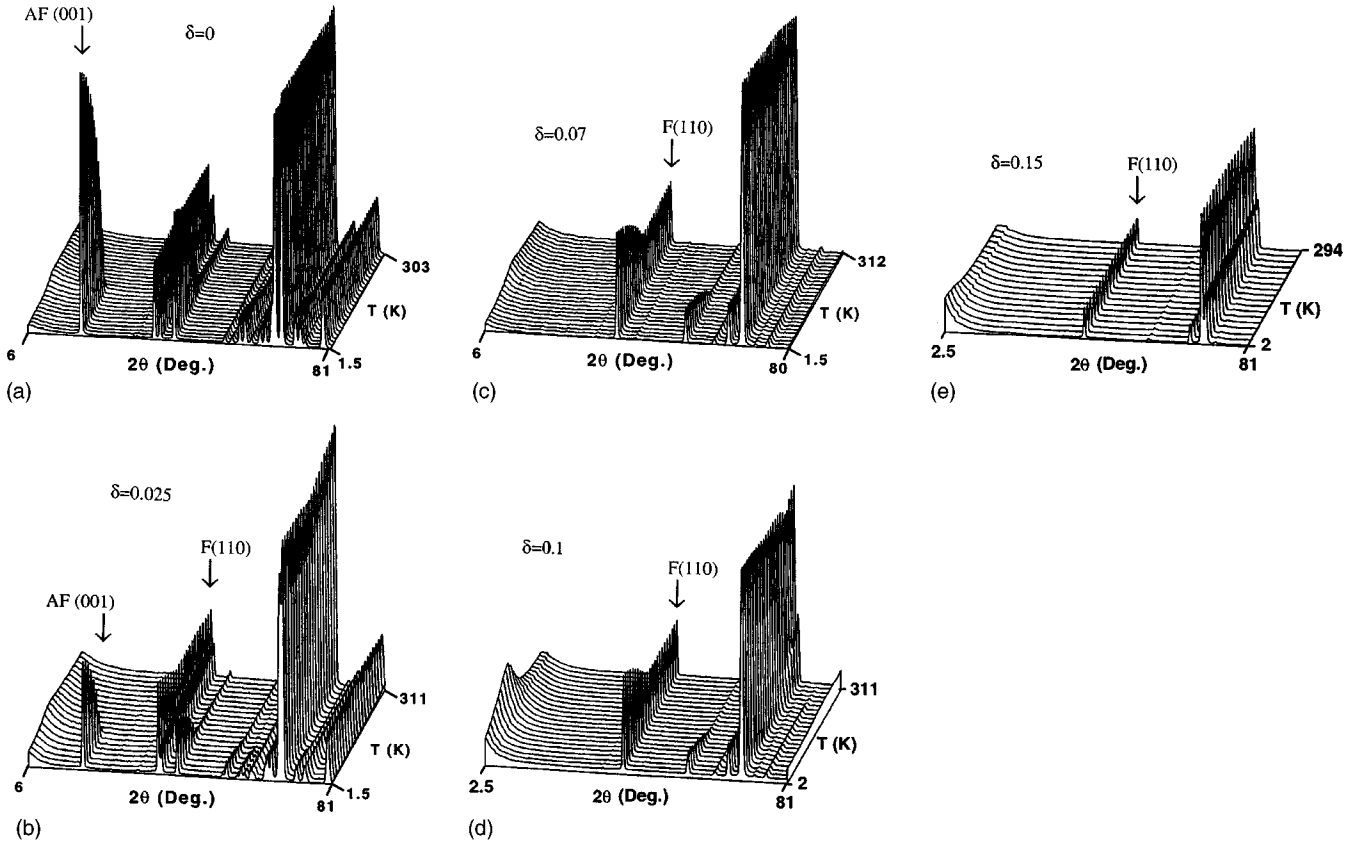
FIG. 3. Neutron thermodiffractograms of (a) $LaMnO_3$, (b) $LaMnO_{3.025}$, (c) $LaMnO_{3.07}$, (d) $LaMnO_{3.1}$, (e) $LaMnO_{3.15}$.

ior may be associated with the presence of Mn vacancies, which reach the value of 4.8% in this compound. It seems that this value approaches the percolation threshold for long-range magnetic order in these compounds. In fact, strong irreversibilities in the field-cooled and zero-field-cooled were observed below 50 K in the thermal dependence of the magnetization as can be observed in Fig. 2(c). As a consequence, the cusplike anomaly at 50 K observed in the χ_{ac} of this compound [see Fig. 2(a)] may be ascribed to the freezing of the spin system. This is in agreement with the results obtained by Hauback, Helmer, and Sakai,[6] which also proposed the existence of a spin-glass state at low temperatures for this compound. We will show in the next section that this is only a simplified picture of a more complex magnetic ground state.

The paramagnetic susceptibility was measured and fitted using a Curie law in the temperature range 200–300 K. The values obtained for the Curie constant C, the paramagnetic Curie temperature, θ_p, and paramagnetic moment are given in Table I. As can be seen from this table, the obtained values are a little high in comparison with the corresponding ionic values ($Mn^{3+} = 4.9\mu_B$ and $Mn^{4+} = 3.8\mu_B$).

C. Neutron diffraction

In order to study the structure and the nature of the magnetic interactions we performed neutron-diffraction experiments between 1.5 and 320 K using three instruments. The temperature dependence of the structural parameters was obtained at the D1B multidetector diffractometer. The samples $\delta = 0.025$ and $\delta = 0.07$ were measured as well at low tem-

peratures at the high-resolution D2B diffractometer. In all cases the data refinements were performed using the Rietveld method by means of the FULLPROF program. The large magnetic contribution to the SANS was measured using the SANS instrument D16.

$\delta = 0$, 0.025, 0.07: orthorhombic structure

All three compounds show orthorhombic structure in the studied range of temperatures. In Figs. 3(a)–3(c) the thermodiffractograms of these compounds are shown. The magnetic structure of the $\delta = 0$ compound was identified by Wollan and Koehler[2] as an antiferromagnetic lattice with ferromagnetic coupling of the Mn ions within the plane (001) and antiferromagnetic interactions between planes. That gives a configuration of alternating ferromagnetic planes having opposite spin directions. In Fig. 3(a) one can notice the presence of extra magnetic peaks below $T_N = 140$ K in this compound. That indicates the existence of long-range antiferromagnetic order. For the $\delta = 0.025$ compound, antiferromagnetic peaks appear at $T_N = 110$ K at the same positions that in the $\delta = 0$ compound [see Fig. 3(b)]. However, the $\delta = 0.025$ compound also shows a ferromagnetic contribution. This result can be explained as due to the coexistence of ferro and antiferromagnetic regions at low temperatures or the existence of a magnetic canted structure. The appearance of the ferromagnetic and antiferromagnetic contributions at the same temperature makes more plausible the existence of a low-temperature antiferromagnetic canted structure. The refinement of the neutron-diffraction data at the lowest temperature gives a value of $1.48\mu_B$ for the ferromagnetic com-
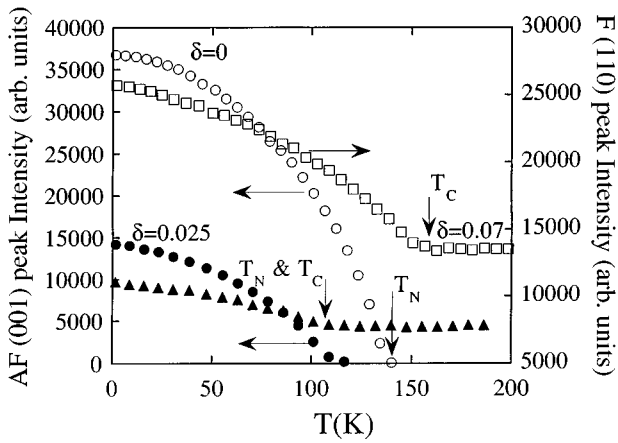
FIG. 4. Thermal dependence of the antiferromagnetic peak (001) in the compounds LaMnO$_3$ and LaMnO$_{3.025}$ and the ferromagnetic peak (110) in the compounds LaMnO$_{3.025}$ and LaMnO$_{3.07}$.

ponent and of 2.52μ_B for the antiferromagnetic component (see Table I). For the $\delta=0.07$ compound, only a very small antiferromagnetic component of 0.25μ_B was found from the refinement of the low-temperature spectrum. A large ferromagnetic contribution is observed below $T_C=160$ K [see Fig. 3(c)], which reaches a value of 3.25μ_B/Mn at the lowest temperature. It can be seen in Table I that this value is in good agreement with the value obtained from magnetization measurements (3.43μ_B/Mn). In Fig. 4 the thermal dependence of the intensity of the main magnetic peaks of these compounds is shown.

From the refinements of the spectra, the thermal dependence of the lattice parameters has been obtained. The linear thermal expansion along the main symmetry directions for the three compounds is shown in Fig. 5. Two different kinds of anomalies can be distinguished. At the magnetic ordering temperatures, T_C or T_N, small kinks exist in the curves. The magnitude of these changes is small and is not related to the large static Jahn-Teller distortion, but to magnetoelastic effects associated with the magnetic phase transitions. However, for the $\delta=0.07$ compound large anomalies can be observed at the same temperature that the abrupt decrease in the susceptibility takes place (≈110 K). In La$_{0.35}$Ca$_{0.65}$MnO$_3$ a large anisotropic lattice effect associated with the charge ordering establishment was found.[13] It seems that the same effect occurs in the $\delta=0.07$ compound. Competition between ferromagnetism and charge ordering is not new in manganese perovskites. For instance, in the La$_{1-x}$Ca$_x$MnO$_3$ system, strong evidence of charge ordering instabilities have been found even below the ferromagnetic ordering temperature.[12,14]

In Fig. 6 we show the obtained values for the Mn-O distances as a function of δ at 1.5 and 300 K. For $\delta=0$ we observe the largest static Jahn-Teller distortion of the octahedra. This distortion remains nearly constant with temperature. For the $\delta=0.025$ compound a small reduction in the Jahn-Teller distortion is observed. The static Jahn-Teller distortion is significantly reduced for the $\delta=0.07$ compound, being almost negligible at 300 K. This constitutes an indication of the instability of the orthorhombic structure for increasing values of δ. Thus, for temperatures above 300 K one may expect the three Mn-O distances to become equal,
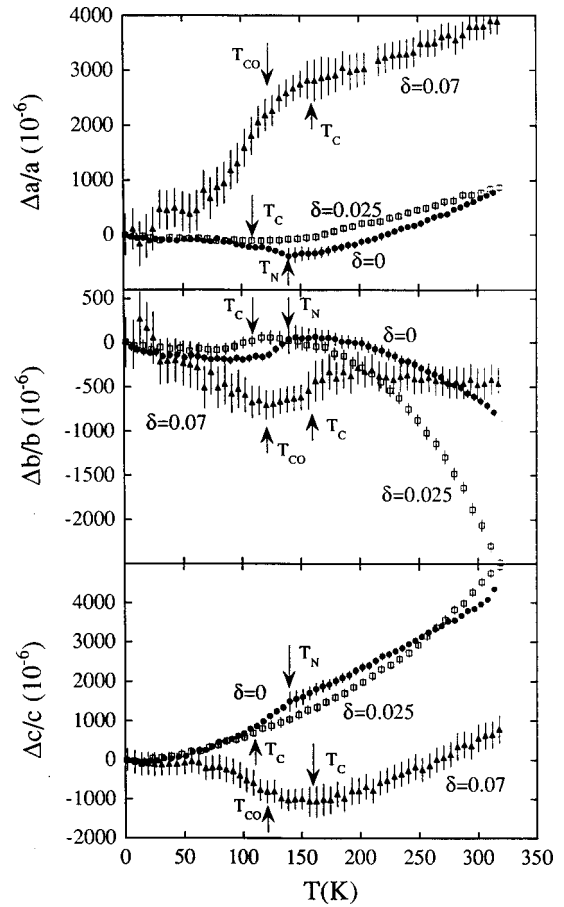

FIG. 5. Thermal expansion of the lattice parameters of LaMnO$_{3+\delta}$ ($\delta\leqslant0.07$) obtained from the Rietveld refinement of the neutron-diffraction spectra.
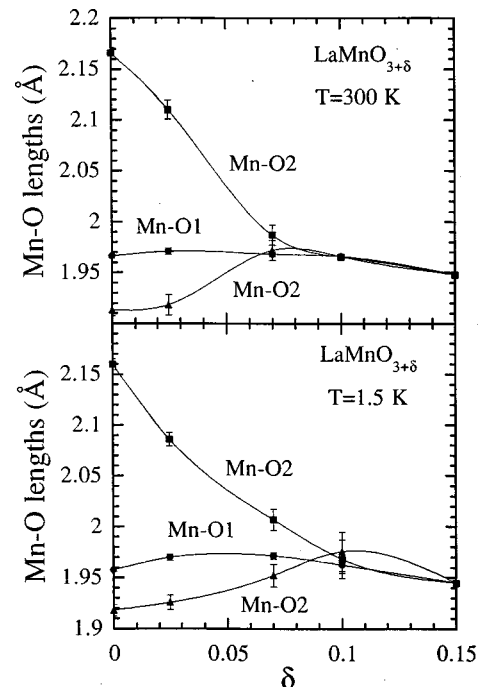

FIG. 6. Mn-O distances obtained from the refinement of the neutron-diffraction results in the LaMnO$_{3+\delta}$ series (lines are visual guides) at $T=1.5$ and 300 K.
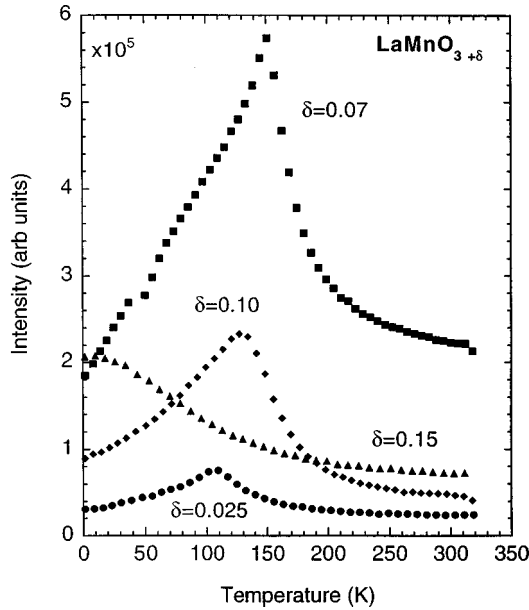
FIG. 7. Thermal dependence of the intensity of the small-angle neutron scattering (SANS) in the series LaMnO$_{3+\delta}$ at $q = 0.13$ Å^{-1}.

$d_{\text{Mn-O}} = 1.96$ Å, and also $a \approx b \approx c/\sqrt{2} \approx 5.5$ Å. This would correspond to a rhombohedral structure, which is indeed the structure found in compounds with higher δ values. The Mn-O-Mn angle as a function of δ has also been obtained at 1.5 and 300 K (not shown here). The smallest Mn-O(1)-Mn and Mn-O(2)-Mn angles correspond to the $\delta = 0$ compound. The increase in the Mn-O-Mn bond angle as δ increases is in accordance with the enhancement of the ferromagnetic interaction. In the $\delta = 0.07$ compound the value obtained for the Mn-O-Mn bond angle ($\approx 170°$) seems to be close to the critical value for the existence of ferromagnetism in these compounds in good agreement with previous results.[8]

We have found a large magnetic contribution to the SANS in this series for $\delta \geqslant 0.07$. In Fig. 7 we show the SANS intensity as a function of temperature at $q = 0.13$ Å^{-1}, which is the lowest available value in the D1B instrument. In addition to the critical scattering, characteristic of the order-disorder magnetic phase transition at T_C, we have found an extra magnetic contribution in the ordered phase. The critical magnetic scattering appears in the neighborhood of T_C as a consequence of the critical fluctuation of the magnetization which gives rise to a diffuse scattering at very low q values. In La$_{2/3}$Ca$_{1/3}$MnO$_3$, a large SANS magnetic contribution in the paramagnetic phase was found.[15] This effect was associated with the existence of magnetic polarons (ferromagnetic clusters in the paramagnetic region associated with a lattice polaron). Unlike this behavior, the $\delta = 0.07$ and $\delta = 0.1$ compounds show a large magnetic contribution to the SANS well below the phase transition temperature, which cannot be related to critical scattering. We have studied the SANS of the $\delta = 0.07$ compound with a more appropriate SANS instrument, D16. In Fig. 8 the obtained results are displayed. In Fig. 8(a) the SANS intensity at different q values is shown. At the lowest available q, 0.036 Å^{-1}, it is clearly observed that together with an increase in the intensity, characteristic of critical scattering at around T_C, an anomalous magnetic contribution appears be-
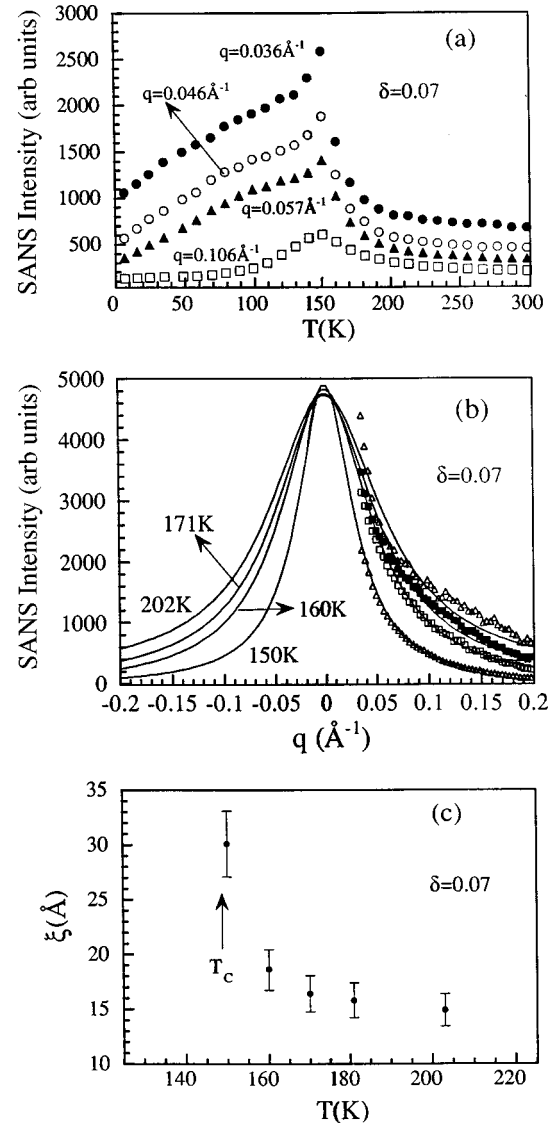

FIG. 8. (a) Thermal dependence of the intensity of the SANS at different momentum transfer values in LaMnO$_{3.07}$. (b) Fits of the magnetic SANS intensity to q dependence of Lorentzian type, $I = I_0/(q^2 + (1/\xi)^2)$, where ξ is the magnetic correlation length, for selected temperatures above T_C. (c) Thermal dependence of ξ obtained from such fits.

low T_C. This effect is more difficult to see for q values larger than ≈ 0.1 Å^{-1}. This indicates that below T_C we are dealing with quite large magnetic coherence length. D16 is appropriate for the study of magnetic clusters of size of some tens of Å. This fact prevented us from obtaining the exact size of the magnetic coherence length below T_C, even though qualitative information can be drawn. In Fig. 8(b) the fits of the magnetic SANS intensity to Lorentzian-type q dependence above T_C are shown. The magnetic SANS intensity was obtained after subtracting from the total SANS intensity the estimated temperature-independent incoherent nuclear scattering. The magnetic correlation length, ξ, as a function of temperature obtained from such fits is shown in Fig. 8(c). At $T_C \sim 150$ K, ξ tends to diverge as expected from the divergence of the magnetic susceptibility at the paramagnetic-ferromagnetic transition temperature. The fits below T_C are not reliable enough to be shown but we can say

TABLE II. Structural data for all the studied compounds.

δ		0	0.025	0.07	0.1	0.15
Mn^{4+} (%)		0	5	14	20	30
Formula unit		LaMnO$_3$	La$_{0.992}$Mn$_{0.992}$O$_3$	La$_{0.977}$Mn$_{0.977}$O$_3$	La$_{0.968}$Mn$_{0.968}$O$_3$	La$_{0.952}$Mn$_{0.952}$O$_3$
Space group						
	1 K	*Pbnm*	*Pbnm*	*Pbnm*	*Pbnm*	*R$\bar{3}$c*
	300 K	*Pbnm*	*Pbnm*	*Pbnm*	*R$\bar{3}$c*	*R$\bar{3}$c*
1 K	a (Å)	5.5330	5.5351	5.5069	5.5109	5.4759
	b (Å)	5.7273	5.6188	5.4948	5.4714	5.4759
	c (Å)	7.6681	7.7157	7.7638	7.7642	13.222
	Vol/z (Å^3)	60.75	60.00	58.73	58.53	57.22^a
300 K	a (Å)	5.5350	5.5394	5.5278	5.5322	5.4814
	b (Å)	5.7230	5.6072	5.4922	5.5322	5.4814
	c (Å)	7.6970	7.7507	7.7681	13.3422	13.261
	Vol/z (Å^3)	60.96	60.18	58.96	58.94	57.51
1 K	Mn-O$_I$	1.9579	1.9697	1.9715	1.9737	1.9449
	Mn-O$_{II}$	2.1597	2.0857	2.0070	1.9684	1.9449
	Mn-O$_{II}$	1.9181	1.9256	1.9523	1.9756	1.9449
300 K	Mn-O$_I$	1.9662	1.9708	1.9683	1.9737	1.9480
	Mn-O$_{II}$	2.1658	2.1100	1.9870	1.9737	1.9480
	Mn-O$_{II}$	1.9134	1.9182	1.9718	1.9737	1.9480
Mn-O$_I$-Mn (1 K)		168.27	168.32	169.89	171.52	172.20
Mn-O$_I$-Mn (300 K)		168.16	169.40	170.63	170.76	172.27
Mn-O$_{II}$-Mn (1 K)		168.22	169.87	169.39	169.89	172.20
Mn-O$_{II}$-Mn (300 K)		168.16	168.64	169.84	170.66	172.27

$^a z = 6$ for $R\bar{3}c$.

that the magnetic coherent length can be around 100 Å in this ferromagnetic phase. This value is lower than in normal ferromagnets. These effects point to an inhomogeneous magnetic ground state in the ferromagnetic phase, which could explain the absence of an insulator-metal transition at the para-ferromagnetic transition.

$\delta = 0.1$: *rhombohedral-orthorhombic transition*

X-ray and neutron-diffraction spectra at room temperature of the $\delta = 0.1$ compound were refined in the $R\bar{3}c$ rhombohedral space group which results in the structural parameters given in Table II. However, the low-temperature neutron-diffraction results were refined in the *Pbnm* orthorhombic space group. The thermal diffractogram in Fig. 3(d) shows that a structural transition takes place below $T_S \approx 300$ K, which is manifested as the disappearance of the characteristic orthorhombic Bragg peak (210)&(120) at this temperature. The thermal dependence of the intensity of this peak is shown in Fig. 9. A small ferromagnetic contribution is observed below $T_C = 150$ K. The thermal dependence of the intensity of the (110) peak is plotted in Fig. 9. From the Rietveld refinement an effective ferromagnetic moment of $2.86\mu_B$ was obtained, which is in good agreement with the

magnetization measurements (see Table I) and rather low in comparison with the expected value for fully polarized Mn magnetic moments. The thermal dependence of the lattice parameters is displayed in the inset of Fig. 10. The large
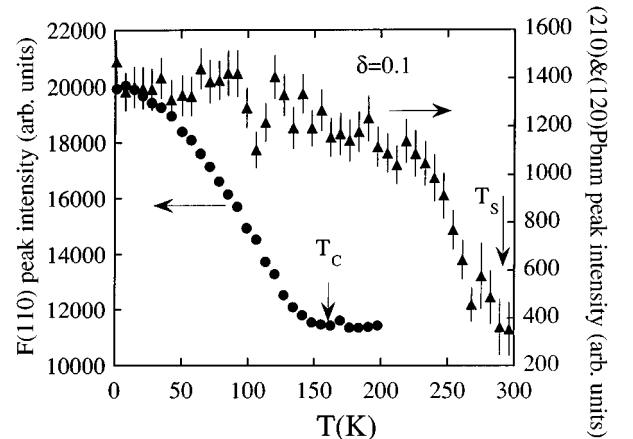

FIG. 9. Thermal dependence of the orthorhombic (210) and (120) structural peak (situated at $2\Theta = 62°$) and the ferromagnetic peak (110) of LaMnO$_{3.1}$.
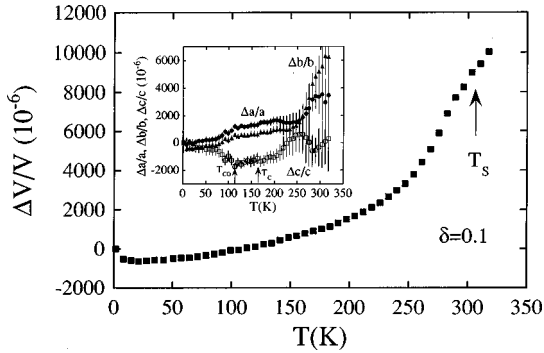
FIG. 10. Volume thermal expansion of LaMnO$_{3.1}$ calculated from the value of the lattice parameters obtained by Rietveld refinement of the neutron-diffraction spectra. The inset shows the thermal dependence of the lattice parameters of LaMnO$_{3.1}$.
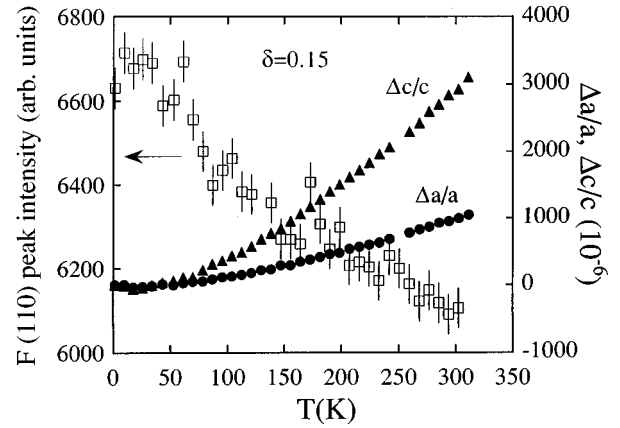

FIG. 11. Thermal dependence of the lattice parameters obtained from the Rietveld refinement of the neutron-diffraction spectra and of the intensity of the ferromagnetic (110) peak in LaMnO$_{3.15}$.

uncertainty in the determination of the lattice parameters at high temperatures (see the large value of the error bars) is a consequence of the structural transition below $T_S \approx 300$ K. Both phases, orthorhombic and rhombohedral, coexist across a certain range of temperature (~ 40 K), which makes the error bars of the fits larger. A huge change in the volume of the sample is observed through the structural transition as can be seen in Fig. 10. In the inset of Fig. 10 one can notice that at $T_C = 150$ K there are not relevant changes in the lattice parameters. However, at $T \sim 110$ K large anomalies are detected in the lattice parameters at the same temperature as the drop in susceptibility takes place. As occurs in the $\delta = 0.07$ compound, this fact is consistent with a charge ordering transition. In Fig. 6 one can see that the $\delta = 0.1$ compound still presents a very small but perceptible distortion of the MnO$_6$ octahedra at 1.5 K reminiscent of the static Jahn-Teller distortion of LaMnO$_3$. This effect is no longer seen at 300 K, above T_S, as a consequence of the transition to the rhombohedral structure in which all Mn-O distances become equal. This compound also shows a significant magnetic contribution to the SANS as can be seen in Fig. 7, which is very important at low temperatures, far below T_C. As occurs in the compound $\delta = 0.07$, this contribution can be ascribed to the existence of magnetic inhomogeneity below T_C. This effect seems to be inherently connected in these compounds to the existence of an insulating state coexisting with the ferromagnetic ordering.

$\delta = 0.15$: *rhombohedral structure*

In this compound the maximum oxygen content, i.e., the largest number of La and Mn vacancies, was obtained. The determined Mn^{4+} concentration by chemical analysis was 30%, which represents 4.8% of La and Mn vacancies, respectively. In Fig. 3(e) the neutron thermodiffractogram obtained for this compound is shown. From room temperature down to 1.5 K the rhombohedral structure was found to be stable. The refinement of the neutron-diffraction spectra at several temperatures gave the thermal dependence of the lattice parameters shown in Fig. 11, where no anomaly was observed. The analysis of the thermal dependence of the intensity of the (110) peak reveals a weak ferromagnetic contribution as shown in Fig. 11. This contribution corresponds to an effective magnetic moment per Mn of $0.97\mu B$ at 1.5 K,

which is much lower than the expected for fully polarized Mn ions. The lack of antiferromagnetic peaks indicates that the weakness of the ferromagnetic contribution which appears below $T_C \sim 150$ K cannot be ascribed to the existence of a canted antiferromagnetic structure. The cusplike anomaly found in χ_{ac} at $T_f = 50$ K [see Fig. 2(a)] and the magnetic irreversibilities observed in the field-cooled and zero-field-cooled magnetization measurements [see Fig. 2(c)] suggest the existence of a disordered cluster-glass state. We can explain this behavior considering that the sample will be very inhomogeneous as a consequence of the large amount of Mn and La vacancies which will bring about strong randomness in the magnetic interactions. Nevertheless, there exists a volume fraction of the sample where the long-range magnetic interaction is possible. The thermal dependence of the SANS intensity at $q = 0.1$ Å^{-1}, as inferred from D1B data, shows a pronounced shoulder at low temperature (see Fig. 7). A similar behavior was found in (La$_{2/3}$Tb$_{1/3}$)$_{2/3}$Ca$_{1/3}$MnO$_3$,[16] which is cluster glass at low temperatures. In order to get an insight into the nature of the low-temperature ground state of this compound we performed SANS measurements in D16. The results are shown in Fig. 12. In Fig. 12(a) the SANS intensity is plotted at different q values as a function of temperature. There is not a sign of critical scattering in agreement with the absence of long-range magnetic order. The thermal dependence of the SANS intensity points to the existence of a cluster-glass magnetic state at low temperatures. The magnetic SANS intensity has been fitted to a Lorentzian function [see some selected fits in Fig. 12(b)]. The magnetic correlation length obtained from such fits is shown in Fig. 12(c). These values represent average sizes for the magnetic clusters, even though a very small magnetic contribution to the Bragg peaks would come from the existence of a few larger clusters.

III. DISCUSSION AND CONCLUSIONS

The wide characterization performed in a series of samples with different δ values has allowed us to draw conclusions that may help to clarify some aspects related to the structural, magnetic, and magnetotransport properties of
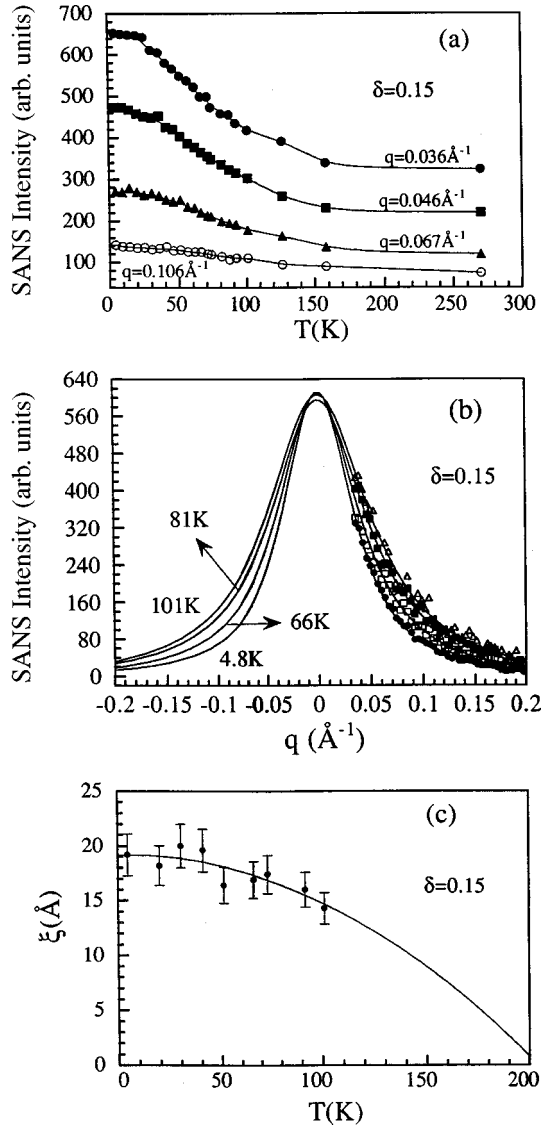
FIG. 12. (a) Thermal dependence of the intensity of the SANS at different momentum transfer values in $LaMnO_{3.15}$. (b) Fits of the magnetic SANS intensity to q dependence of Lorentzian type, $I = I_0 / [q^2 + (1/\xi)^2]$, where ξ is the magnetic correlation length, for selected temperatures. (c) Thermal dependence of ξ obtained from such fits.

$LaMnO_{3+\delta}$ (for $\delta \leqslant 0.15$). Similar results were obtained on samples of the same concentration prepared at different laboratories using different methods of preparation. A careful chemical analysis was performed, giving concentrations equal to the nominal one within the experimental error. The structural and magnetic behavior was found to change systematically through the series. Hauback, Helmer, and Sakai[6] reported the existence of two orthorhombic phases ORT1 and ORT2. The ORT1, found for $LaMnO_3$, where the a and c lattice parameters (using the *Pnma* nomenclature) are different, reflecting the large Jahn-Teller distortion of the $Mn^{3+}O_6$ octahedra and the ORT2, observed for $\delta = 0.07$, where $a \approx c$. Our x-ray and neutron-diffraction spectra were refined in the *Pbnm* space group, with the a and c axis of *Pnma* becoming the b and a axis. In Table II we show the variation of a and b through the series. As δ increases a and b become closer. This evolution reflects a trend, which is also followed by the distortion of the MnO_6 octahedra as shown in Fig. 6. These results constitute an indication of the breakdown of the coherence associated with the cooperative Jahn-Teller effect in $LaMnO_3$ as δ increases. This behavior is also observed in substituted mixed-valence manganites like $La_{1-x}Ca_xMnO_3$,[2] where as x increases the static distortion is disfavored. In both series this distortion is drastically reduced under the effect of the increase in Mn^{4+} ions concentration. From these results we can conclude that the strict division into two different crystallographic phases, ORT1 and ORT2, is not justified as there is a continuous change from highly distorted orthorhombic towards quasicubic (in $LaMnO_{3.07}$ $a \approx b \approx c/\sqrt{2}$) and then rhombohedral structure through the series as δ increases.

The analysis of the neutron diffraction provides detailed information about the structure and magnetic behavior. A correlation between a given crystallographic structure and the magnetic state must be ruled out after our study. However, we observed a progressive weakening of the antiferromagnetic interaction and an enhancement of the ferromagnetic one. This trend is clearly shown in Table I up to $\delta = 0.07$. For higher δ concentration the ferromagnetic interaction starts to decrease for increasing δ values. The increase in the ferromagnetic interaction up to $\delta = 0.07$ can be explained by the increase in both the Mn^{4+} ions concentration and the Mn-O-Mn bond angle, which favor the Mn^{4+}-O^{2-}-Mn^{3+} double exchange interaction. Another fact that can account for this behavior is the enhancement of the Mn^{3+}-O^{2-}-Mn^{3+} ferromagnetic contribution as a consequence of the induced vibronic Jahn-Teller effect as proposed by Goodenough *et al.*[17] and recently discussed by Dionne.[18] This would agree with the loss of coherence (namely, decrease in the static octahedra distortion) in regard to the static case, $\delta = 0$, in which both interactions, the Mn^{3+}-O^{2-}-Mn^{3+} ferromagnetic within the (001) planes and the antiferromagnetic Mn^{3+}-O^{2-}-Mn^{3+} along the c axis coexist. For δ values larger than 0.07 the ferromagnetic moment decreases again evolving from $3.25\mu_B$ for $\delta = 0.07$ down to $0.78\mu_B$ at $\delta = 0.15$. We associate this effect with the increasing number of Mn vacancies which block the ferromagnetic interaction. The crucial role of the Mn vacancies in the destruction of the long-range ferromagnetic order can be seen in the $\delta = 0.15$ compound, where in fact cluster-glass behavior is found below ≈ 40 K. The existence of a residual spontaneous ferromagnetic moment below $T_C \sim 160$ K in the $\delta = 0.15$ compound suggests the coexistence of both states: a small part of the sample with long-range magnetic order (large clusters) and the major part with a cluster-glass magnetic state. This hypothesis is strongly supported by the small-angle neutron-scattering results. The SANS results indicate the absence of a true para-ferromagnetic transition but the existence of magnetic clusters at low temperature of size around 20 Å. The large magnetoresistance effect in this compound can be ascribed to the effect of the magnetic field on the cluster-glass regions of the sample. A similar behavior in magnetoresistance was found in the cluster-glass compound $(La_{2/3}Tb_{1/3})_{2/3}Ca_{1/3}MnO_3$.[16] The insulator state observed in the ferromagnetic samples, $\delta = 0.07$ and $\delta = 0.1$, is unusual. One important intrinsic property of these compounds observed with the SANS experiments is the existence of the magnetic contribution to the SANS in the ferromagnetic

phase. This points to smaller magnetic coherence length than in a typical ferromagnet. Magnetic inhomogeneity seems to exist in the ferromagnetic region. However, we do not rule out that the grain-boundary resistivity, which has been found to be very important in related compounds,[19] can mask the true intrinsic resistivity behavior.

Another remarkable result found in the $\delta = 0.07$ and $\delta = 0.1$ compounds is the existence of magnetic and structural features that point to the existence of charge-ordered regions at temperatures below ~ 110 K, well below the ferromagnetic ordering temperature. The ground state in these compounds is proposed to be a coexistence of ferromagnetic and charge-ordered regions. The insulator behavior in these compounds would be explained by the coexistence of not too large (~ 100 Å) ferromagnetic clusters (seen by SANS experiments) and insulating charge-ordered regions.

In the $\delta = 0.1$ compound an orthorhombic-rhombohedral transition has been detected at around room temperature that brings about a huge change in volume. The rhombohedral structure is stable in the $\delta = 0.15$ compound across the whole range of temperatures studied.

Summarizing, in this work we have performed a systematic study of LaMnO$_{3+\delta}$ (for $\delta \leq 0.15$) with the aim at advancing the knowledge of the underlying mechanisms which drive the structural, magnetic, and magnetotransport properties in the LaMnO$_{3+\delta}$ compounds. From the analysis of the experimental results we can conclude:

(i) Through the series, as δ increases, a continuous evolution of the highly distorted orthorhombic structure in LaMnO$_3$ towards quasicubic and then rhombohedral at $\delta = 0.15$ takes place. In the compound $\delta = 0.1$ an orthorhombic-rhombohedral transition with a huge change in volume occurs at around room temperature.

(ii) The magnetic order is not related to a special crystallographic structure. Antiferromagnetic and ferromagnetic ordering are found in the orthorhombic structure and ferromagnetism and spin-glass behavior in the rhombohedral structure.

(iii) The existence of an equal amount of La and Mn vacancies for $\delta \leq 0.07$, results in an enhancement of the ferromagnetic interaction. For $\delta \geq 0.07$ the breakdown of the long-range magnetic interactions gives rise to the formation of magnetic clusters that can explain the ferromagnetic insulator state found in these compounds. In the intermediate compounds $\delta = 0.07$ and $\delta = 0.1$, features characteristic of charge-ordered regions have been detected.

(iv) These compounds do not present a large magnetoresistance effect except for the compound $\delta = 0.15$, for which there is not a spontaneous insulator-metal transition, but magnetoresistance ratios of 10^4 were induced by applying 12 T.

*Author to whom correspondence should be addressed: M. R. Ibarra, Departamento de Física de la Materia Condensada and Instituto de Ciencia de Materiales de Aragón, Universidad de Zaragoza and Consejo Superior de Investigaciones Científicas, Facultad de Ciencias, 50009-Zaragoza, Spain. Electronic mail: ibarra@posta.unizar.es, Fax-3476761229.

[1] G. H. Jonker and J. H. van Santen, Physica (Amsterdam) **16**, 337 (1950).

[2] E. O. Wollan and W. C. Koehler, Phys. Rev. **100**, 545 (1955).

[3] J. B. Goodenough, Phys. Rev. **100**, 564 (1955).

[4] B. C. Tofield and W. R. Scott, J. Solid State Chem. **10**, 183 (1974).

[5] J. A. M. van Roosmalen and E. H. P. Cordfunke, J. Solid State Chem. **110**, 109 (1994).

[6] B. C. Hauback, F. Helmer, and N. Sakai, J. Solid State Chem. **124**, 43 (1996).

[7] C. N. R. Rao and A. K. Cheetham, Science **272**, 369 (1996).

[8] R. Mahendiran, S. K. Tiwary, A. K. Raychaudhuri, T. V. Ramakrishnan, R. Mahesh, N. Rangavittal, and C. N. R. Rao, Phys. Rev. B **53**, 3348 (1996).

[9] A. K. Cheetham, C. N. R. Rao, and T. Vogt, J. Solid State Chem. **126**, 337 (1996).

[10] A. Arulraj, R. Mahesh, G. N. Subbana, R. Mahendiran, A. K. Raychaudhuri, and C. N. R. Rao, J. Solid State Chem. **127**, 87 (1996).

[11] J. Töpfer, J.-P. Doumerc, and J-C. Grenier, J. Mater. Chem. **6**, 1511 (1996).

[12] S.-W. Cheong, C. M. López, and H. Y. Hwang (unpublished).

[13] M. R. Ibarra, J. M. De Teresa, J. Blasco, P. A. Algarabel, C. Marquina, J. García, J. Stankiewicz, and C. Ritter, Phys. Rev. B **56**, 8252 (1997).

[14] P. Schiffer, A. P. Ramirez, W. Bao, and S.-W. Cheong, Phys. Rev. Lett. **75**, 3336 (1995).

[15] J. M. De Teresa, M. R. Ibarra, C. Marquina, P. A. Algarabel, J. Blasco, J. García, Z. Arnold, K. Kamanev, C. Ritter, and R. von Helmolt, Phys. Rev. B **54**, 1187 (1996).

[16] J. M. De Teresa, M. R. Ibarra, J. García, J. Blasco, C. Ritter, P. A. Algarabel, C. Marquina, and A. del Moral, Phys. Rev. Lett. **76**, 3392 (1996).

[17] J. B. Goodenough, A. Wold, N. Menyuk, and R. J. Arnott, Phys. Rev. **124**, 373 (1961).

[18] G. F. Dionne (unpublished).

[19] H. Y. Hwang, S-W. Cheong, N. P. Ong, and B. Batlogg, Phys. Rev. Lett. **77**, 2041 (1996).